

## Assignments of Several Groups of Iodine ( $I_2$ ) Lines in the $B-X$ System

S. GERSTENKORN AND P. LUC

*Laboratoire Aimé Cotton, CNRS II, Bâtiment 505, 91405 Orsay, France*

The spectra obtained by means of Fourier spectroscopy and the assignments of the  $B-X$  lines of  $I_2$  in the vicinity of two argon ion laser lines (5145 and 5287 Å), three krypton ion laser lines (5208, 5308, and 5683 Å), and one He-Ne laser line (6119 Å) are given. A detailed comparison, in the vicinity of the argon ion laser line (5145 Å), between the iodine wavenumbers calculated by means of the two sets of molecular constants previously published [Wei and Tellinghuisen, *J. Mol. Spectrosc.* 50, 317–332 (1974); Barrow and Yee, *J. C. S. Faraday II*, 69, 684–700 (1973)] with those calculated from Fourier spectroscopy data, is presented.

### 1. INTRODUCTION

Since the recording of the iodine absorption spectrum by means of Fourier spectroscopy, and its publication as an Atlas (1), there was much interest expressed in the assignments of small portions of spectra located near some  $Ar^+$ ,  $Kr^+$ , and He-Ne laser lines. Indeed, these laser radiations are often used to produce excited resonance fluorescence of the visible system of iodine ( $B^3\Pi_{0+} - X^1\Sigma_g^+$ ), or to resolve the hyperfine structure of iodine lines and, more recently, to induce stimulated emission in the optically pumped iodine molecule itself (2–4). We therefore present here detailed assignments of small portions of the iodine absorption spectrum in the vicinity of two argon ion laser lines  $\lambda = 5145$  Å (19 429  $cm^{-1}$ ),  $\lambda = 5287$  Å (18 908  $cm^{-1}$ ), three krypton ion laser lines,  $\lambda = 5208$  Å (19 192  $cm^{-1}$ ),  $\lambda = 5308$   $cm^{-1}$  (18 830  $cm^{-1}$ ),  $\lambda = 5683$  Å (17 594  $cm^{-1}$ ), and one He-Ne laser line  $\lambda = 6119$  Å (16 340  $cm^{-1}$ ). These identified small portions of the iodine spectrum are also given here to show the progress achieved in the assignments of the iodine lines, and to serve as an illustration of the accuracy of the molecular constants describing the entire  $B-X$  system of  $I_2$  (5).

### 2. PROCEDURE USED FOR THE LINE ASSIGNMENTS

A detailed description of the rotational analysis of a typical band (the 30, 0 band) was published in 1977 (6). Starting from previously available constants (7–10), we begin to identify lines belonging to a given band. Of course, discrepancies between our observed wavenumbers and those calculated by means of these previous constants always occur. Fortunately, these discrepancies—nearly constant at the head of the bands—increase continuously, with increasing  $J$ . The identification of the lines is also based on the intensities of the lines and the “doublet” separation as explained in Ref. (6). When a sufficient number of iden-

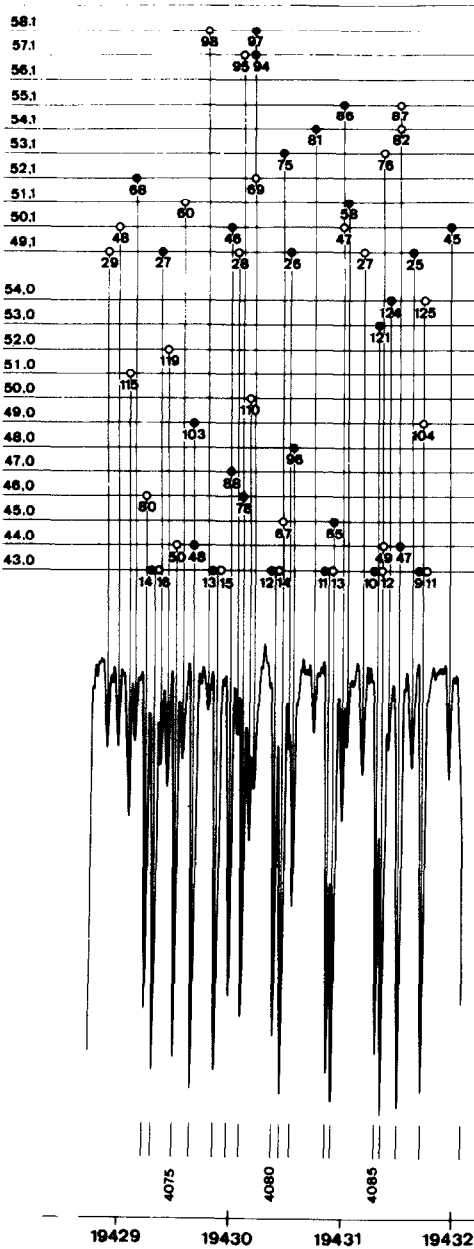


TABLE I

Observed and Calculated Wavenumbers around  $\sigma = 19\,429\text{ cm}^{-1}$  ( $\text{Ar}^+$ ,  $\lambda = 5145\text{ \AA}$ )

N°	$\sigma$ (cm <sup>-1</sup> )	I	Assignments	$\sigma$ (cm <sup>-1</sup> )
Atlas	(observed)			(calculated)
	19428.8372	18	29R (49, 1)	19428.8333
	.9350	18	48R (50, 1)	.9361
	19429.0317	30	115R (51, 0)	19429.0268
	.0830	17	68P (52, 1)	.0798
4073	.1831	63	80R (46, 0)	.1837
4074	.2612	74	14P (43, 0)	.2582
			16R (43, 0)	.2679
	.3184	21	27P (49, 1)	.3160
	.3770	25	119R (52, 0)	.3965
4075	.4501	72	50R (44, 0)	.4491
	.5085	20	60R (51, 1)	.5088
4076	.6064	77	48P (44, 0)	.6040
			103P (49, 0)	.6156
	.7382	12	98R (58, 1)	.7359
4077	.8204	74	13P (43, 0)	.8157
			15R (43, 0)	.8250
4078	.9343	61	46P (50, 1)	.9267
			88P (47, 0)	.9362
4079	.9997	16	28R (49, 1)	19430.0020
	19430.0505	64	78P (46, 0)	.0505
			95R (57, 1)	.0617
	.1107	34	110R (50, 0)	.1069
	.1491	25	69R (52, 1)	.1457
			94P (57, 1)	.1506
			97P (58, 1)	.1634
4080	.3385	68	12P (43, 0)	.3361
			14R (43, 0)	.3449
			75P (53, 1)	.3821
4081	.4123	78	67R (45, 0)	.4095
	.4652	18	26P (49, 1)	.4669
4082	.5036	45	96P (48, 0)	.5042
	.5418	10	104R (61, 1)	.5316
	.6885	16	81P (54, 1)	.6844
4083	.8226	74	11P (43, 0)	.8193
			13R (43, 0)	.8276
4084	.8726	79	65P (45, 0)	.8713
	.9426	31	47R (50, 1)	.9400
			86P (55, 1)	.9457
	.9666	18	58P (51, 1)	.9665
	19431.1313	22	27R (49, 1)	19431.1290
4085	.2653	71	10P (43, 0)	.2654
			121P (53, 0)	.2680
			12R (43, 0)	.2731
4086	.3197	81	49R (44, 0)	.3169
			76R (53, 1)	.3202
			87R (55, 1)	.4577
4087	.4689	80	47P (44, 0)	.4668
			82R (54, 1)	.4347
4088	.5757	21	25P (49, 1)	.5763
	.6779	77	9P (43, 0)	.6743
			104R (49, 0)	.6747
			11R (43, 0)	.6814
	.9099	23	45P (50, 1)	.9071

FIG. 1. Assignments of the iodine absorption lines in the vicinity of the Ar<sup>+</sup> laser line  $\lambda = 5145\text{ \AA}$  ( $\sigma = 19\,429\text{ cm}^{-1}$ ).

tified lines is obtained, we then recalculate the molecular constants describing the band under investigation by a least-squares procedure (nonlinear SIMPLEX). Using these new molecular constants we extend the identification process to higher  $J$  transitions; in general, three iterations were enough to identify lines not buried in

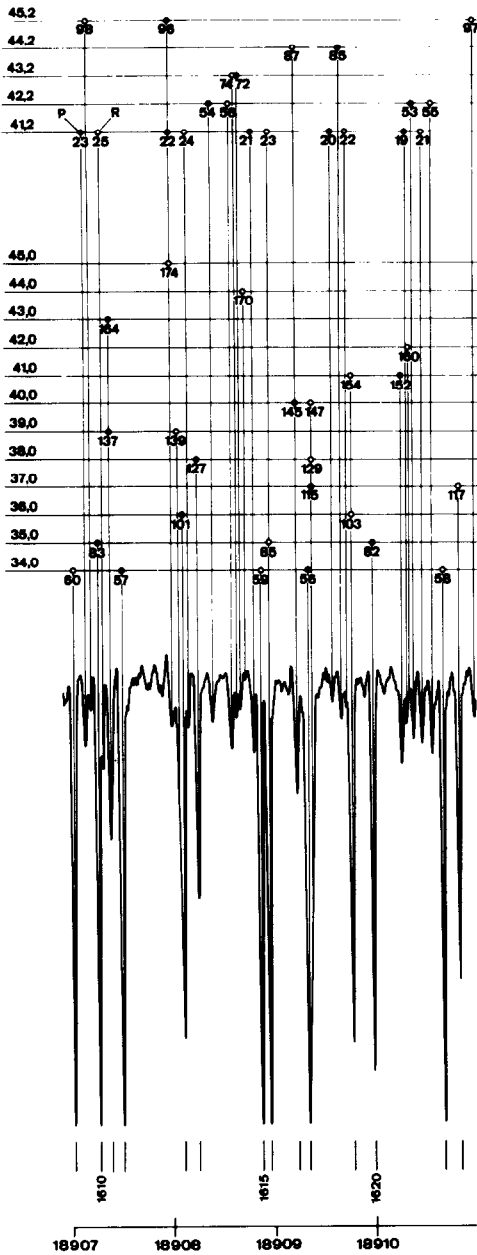


FIG. 2. Assignments of the iodine absorption lines in the vicinity of the  $\text{Ar}^+$  laser line  $\lambda = 5287 \text{ \AA}$  ( $\sigma = 18\,908 \text{ cm}^{-1}$ ).

TABLE II

Observed and Calculated Wavenumbers around  $\sigma = 18\,908 \text{ cm}^{-1}$  ( $\text{Ar}^+$ ,  $\lambda = 5287 \text{ \AA}$ )

N°	$\sigma$ ( $\text{cm}^{-1}$ )	I	Assignments	$\sigma$ ( $\text{cm}^{-1}$ )
Atlas	(observed)			(calculated)
1609	18907.0140	81	60R (34,0)	18907.0113
	.1327	17	23P (41,2)	.1284
	.1888	10	98R (45,2)	.1889
1610	.2582	84	83P (35,0)	.2555
	.2988	21	25R (41,2)	.2996
1611	.3739	35	164P (43,0)	.3609
			137P (39,0)	.3714
1612	.4929	85	57P (34,0)	.4857
	.5503	10		
	.7415	6		
	.7788	6		
	.8622	7		
	.8916	7		
	.9800	13	22P (41,2)	.9795
			174R (45,0)	.9927
			96P (45,2)	18908.0108
			139R (39,0)	.0510
1613	18908.0900	72	101P (36,0)	.0889
	.1449	13	24R (41,2)	.1442
	.2378	46	127P (38,0)	.2360
1614	.3866	12	54P (42,2)	.3875
	.5722	17	56R (42,2)	.5707
	.6240	11	74R (43,2)	.6260
	.6611	12	72P (43,2)	.6635
	.7946	18	21P (41,2)	.7954
1615	.8623	87	59R (34,0)	.8550
1616	.9427	83	85R (35,0)	.9399
			23R (41,2)	.9533
	18909.1426	7		
1617	.2195	26	145P (40,0)	18909.2188
			87R (44,2)	.2776
1618	.3250	80	56P (34,0)	.3193
			115P (37,0)	.3477
			147R (40,0)	.3490
			129R (38,0)	.3739
	.5731	8	20P (41,2)	.5757
	.6618	12	85P (44,2)	.6566
1619	.7674	74	22R (41,2)	.7270
			103R (36,0)	.7666
			154R (41,0)	.7927
	.8980	8		
1620	.9731	79	82P (35,0)	.9732
	18910.0941	7		
	.2655	20	152P (41,0)	18910.2890
	.3136	13	19P (41,2)	.3207
			160R (42,0)	.3445
	.3801	16	53P (42,2)	.3781
	.4665	16	21R (41,2)	.4653
	.5660	18	55R (42,2)	.5601
1621	.6702	85	58R (34,0)	.6669
	.7300	7		
1622	.8281	62	117R (37,0)	.8264
	.9849	11	97R (45,2)	.9896

the noise present in our spectrogram (lines with a signal to noise greater than 4). In this way we identified nearly the entire iodine absorption spectrum observed under our experimental conditions (I). Figures 1 and 2 show the iodine spectrum in the vicinity of the two argon ion laser lines and Tables I and II give the observed

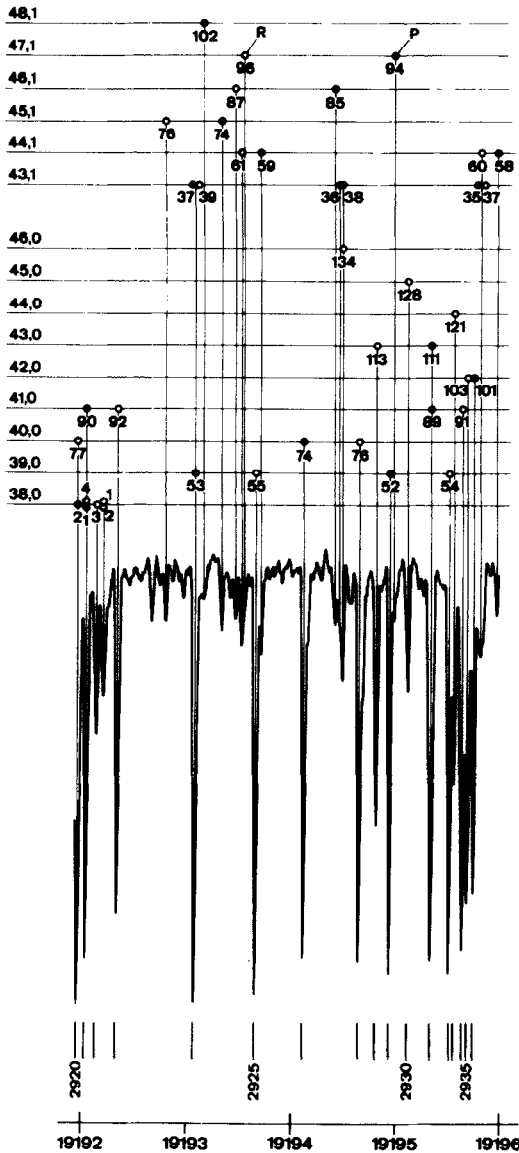


TABLE III

Observed and Calculated Wavenumbers around  $\sigma = 19\ 192\ \text{cm}^{-1}$  ( $\text{Kr}^+$ ,  $\lambda = 5208\ \text{\AA}$ )

N°	$\sigma$ (cm <sup>-1</sup> )	I	Assignments	$\sigma$ (cm <sup>-1</sup> )
Atlas	(observed)			(calculated)
2920	19191.9229	84	77R (40,0)	19191.9197
			2P (38,0)	.9564
2921	19192.0036	76	90P (41,0)	19192.0038
			4R (38,0)	.0064
			1P (38,0)	.0648
2922	.1024	36	3R (38,0)	.1005
	.1639	28	2R (38,0)	.1608
2923	.2978	68	1R (38,0)	.1874
	.6235	15	92R (41,0)	.2984
	.6965	8		
	.7577	15	76R (45,1)	.7573
	.8250	8		
	.9267	11		
2924	19193.0456	84	37P (43,1)	19193.0206
			39R (43,1)	.0340
			53P (39,0)	.0404
	.1225	11	102P (48,1)	.1344
	.2922	16	74P (45,1)	.2912
	.3760	11		
	.4275	14	87R (46,1)	.4299
	.4854	19	61R (44,1)	.4806
			96R (47,1)	.5141
2925	.6285	83	55R (39,0)	.6242
	19193.6740	21	59P (44,1)	.6729
2926	19194.0855	76	74P (40,0)	19194.0842
	.2565	7		
	.3844	15	85P (46,1)	.3837
			36P (43,1)	.4277
			38R (43,1)	.4506
	.4593	25	134R (46,0)	.4750
	.5329	11		
2927	.6176	77	76R (40,0)	.6166
2928	.7853	52	113R (43,0)	.7848
	.8304	9	147R (49,0)	.8355
2929	.9152	79	52P (39,0)	.9134
	.9555	15	94P (47,1)	.9545
2930	19195.0859	27	128R (45,0)	19195.0884
	.1983	9		
2931	.3130	76	111P (43,0)	.3011
			89P (41,0)	.3167
			103R (48,1)	.4691
2932	.4886	79	54R (39,0)	.4884
2933	.5354	44	121R (44,0)	.5324
2934	.6147	75	91R (41,0)	.6145
2935	.6618	66	103R (42,0)	.6607
			75R (45,1)	.6813
2936	.7214	64	101P (42,0)	.7209
	.7684	20	60R (44,1)	.7609
	.7906	21	35P (43,1)	.7975
			37R (43,1)	.8209
	.9463	13	58P (44,1)	.9470

FIG. 3. Assignments of the iodine absorption lines in the vicinity of the Kr<sup>+</sup> laser line  $\lambda = 5208\ \text{\AA}$  ( $\sigma = 19\ 192\ \text{cm}^{-1}$ ).

and calculated wavenumbers. Figures 3, 4, 5, and Tables III, IV, and V present the same data for the three krypton lines, and Fig. 6 and Table IV for the He-Ne laser line. The calculated wavenumbers given in these tables are those obtained from the molecular constants determined by the band-by-band studies. The next step, obtaining the most adequate spectroscopic constants capable of reproducing the iodine spectrum within experimental errors, was then undertaken: the first results

TABLE IV

Observed and Calculated Wavenumbers around  
 $\sigma = 18\,830\text{ cm}^{-1}$  ( $\text{Kr}^+$ ,  $\lambda = 5308\text{ \AA}$ )

Atlas	N°	$\sigma\text{ (cm}^{-1}\text{)}$	I	Assignments	$\sigma\text{ (cm}^{-1}\text{)}$
					(calculated)
	1277	18830.0722	88	65P (33,0)	18830.0662
	1278	.1329	85	17R (32,0)	.1281
				14P (32,0)	.1472
				46P (40,2)	.1745
	1279	.5159	61	110R (35,0)	.5162
	1280	.6000	79	16R (32,0)	.5951
				48R (40,2)	.6094
				13P (32,0)	.6128
	1281	.8629	44	124R (36,0)	.8629
				123R (46,2)	.8881
	1282	18831.0546	84	15R (32,0)	18831.0520
				12P (32,0)	.0484
				92R (34,0)	.0579
				108R (44,2)	.0614
		.3884	12	84P (42,2)	.3933
		.4500	78	14R (32,0)	.4387
				11P (32,0)	.4539
				86R (42,2)	.5344
	1284	.5648	32	143P (38,0)	.5635
		.6141	9	116R (45,2)	.6133
				106P (44,2)	.7565
	1285	.7711	86	67R (33,0)	.7672
	1286	.8231	87	45P (40,2)	.812
				13R (32,0)	.8154
				10P (32,0)	.8293
				98R (43,2)	.8803
	1287	.9297	81	89P (34,0)	.9269
				68P (41,2)	.9472
	1288	18832.0405	73	107P (35,0)	18832.0381
				96P (43,2)	.0996
	1289	.1188	86	64P (33,0)	.1156
				133P (37,0)	.1157
	1290	.1661	81	12R (32,0)	.1619
				9P (32,0)	.1746
		.2423	20	47R (40,2)	.2397
		.3292	13	70R (41,2)	.3279
	1291	.4846	76	11R (32,0)	.4784
				8P (32,0)	.4899
		.6123	24	145R (38,0)	.6105
		.6888	8	121P (46,2)	.6774
	1292	.7697	74	10R (32,0)	.7647
				7P (32,0)	.7750
				114P (45,2)	.8117
	1293	18833.0252	73	9R (32,0)	18833.0210
				6P (32,0)	.0301
	1294	.1395	55	121P (36,0)	.1386
	1295	.2504	68	8R (32,0)	.2471
				5P (32,0)	.2551
				44P (40,2)	.4154
		.4465	66	7R (32,0)	.4432
				4P (32,0)	.4500
	1296	.6136	69	6R (32,0)	.6092
				3P (32,0)	.6149
				135R (37,0)	.6180
	1298	.7481	59	5R (32,0)	.7451
				2P (32,0)	.7496
	1299	.7951	85	66R (33,0)	.7932
	1300	.8487	50	46R (40,2)	.8350
				4R (32,0)	.8510
				1P (32,0)	.8543
		.9568	85	3R (32,0)	.9267
				91R (34,0)	.9337
				151P (39,0)	.9375

FIG. 4. Assignments of the iodine absorption lines in the vicinity of the  $\text{Kr}^+$  laser line  $\lambda = 5308\text{ \AA}$  ( $\sigma = 18\,830\text{ cm}^{-1}$ ).

of this global fit and Dunham expansions of the molecular constants have been given at a recent conference (5).

### 3. COMPARISON WITH PREVIOUSLY PUBLISHED ASSIGNMENTS

Previously published adequately reliable assignments which can be compared with the ones obtained from our studies are available only for three of the six small

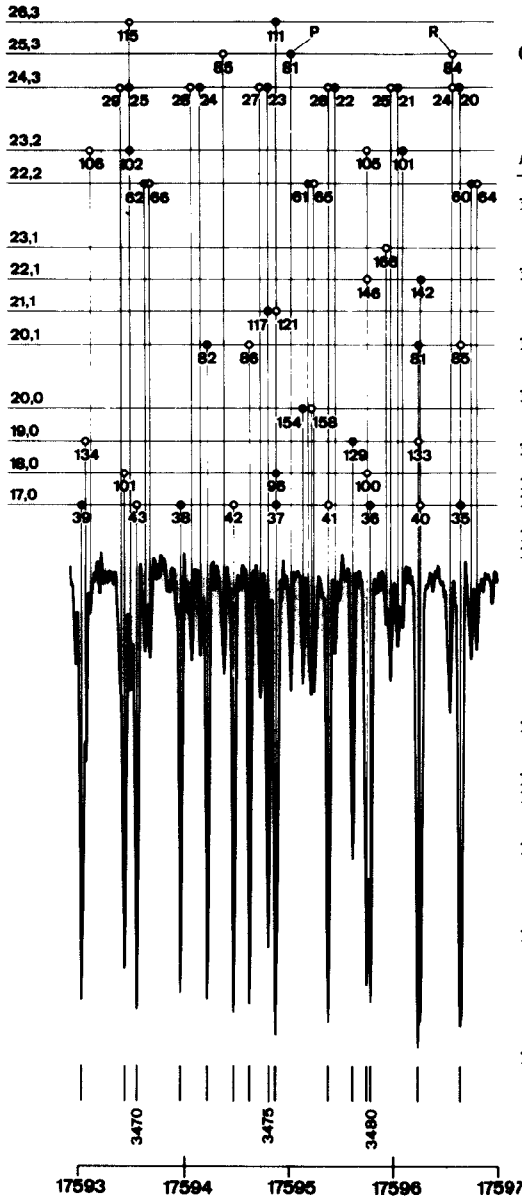


TABLE V

Observed and Calculated Wavenumbers around  $\sigma = 17\,594\text{ cm}^{-1}$  ( $\text{Kr}^+$ ,  $\lambda = 5683\text{ \AA}$ )

N°	$\sigma$ (cm <sup>-1</sup> )	I	Assignments	$\sigma$ (cm <sup>-1</sup> )
Atlas	(observed)			(calculated)
3468	17593.0277	85	39P (17,0)	17593.0285
	.0697	39	134R (19,0)	.0656
3469	.4331	78	106R (23,2)	.1073
			29R (24,3)	.3928
			101R (18,0)	.4318
3470	.5498	86	102P (23,2)	.4710
			25P (24,3)	.4859
			115R (26,3)	.5046
3471	.6318	18	43R (17,0)	.5484
			62P (22,2)	.6292
3472	.6794	20	66R (22,2)	.6785
			96R (17,0)	.9680
3473	17594.0743	20	28R (24,3)	17594.0748
			1575	.1622
3474	.2243	85	82P (20,1)	.2242
			3848	.3820
3475	.4766	86	42R (17,0)	.4761
			6276	.6284
3476	.7330	27	27R (24,3)	.7315
			.8076	.8042
3477	.8772	91	117P (21,1)	.8750
			23P (24,3)	.8154
3478	.9687	83	96P (18,0)	.8829
			111P (26,3)	.8863
3479	17595.0227	26	121R (21,1)	.8848
			81P (25,3)	.8850
3480	.1355	24	154R (20,0)	.1358
			.2166	.2011
3481	.2460	26	61P (22,2)	.2274
			.3808	.2511
3482	.4457	19	26R (24,3)	.3650
			.6092	.3810
3483	.7418	82	41R (17,0)	.4433
			129P (19,0)	.6084
3484	.7812	85	105R (23,2)	.7354
			146R (22,1)	.7394
3485	.9504	13	100R (18,0)	.7421
			36P (17,0)	.7791
3486	.9730	24	166R (23,1)	.9544
			25R (24,3)	.9693
3487	17596.0448	17	21P (24,3)	17596.0460
			.0896	.0910
3488	.2318	93	101P (23,2)	.2321
			133R (19,0)	.2376
3489	.5446	30	81P (20,1)	.2585
			142P (22,1)	.2631
3490	.6352	89	40R (17,0)	.5348
			84R (25,3)	.5503
3491	.7481	60P	24R (24,3)	.6236
			.7850	.6396
3492	.8076	74	20P (24,3)	.6505
			.8772	.7483
3493	.9687	83	85R (20,1)	.7991
			39P (17,0)	
3494	17597.0277	85	60P (22,2)	
			64R (22,2)	

FIG. 5. Assignments of the iodine absorption lines in the vicinity of the Kr<sup>+</sup> laser line  $\lambda = 5683\text{ \AA}$  ( $\sigma = 17\,594\text{ cm}^{-1}$ ).

portions given here: the region around  $19\,429.8\text{ cm}^{-1}$  ( $5145\text{ \AA}$ , Ar<sup>+</sup> laser), investigated by a great number of authors [(11, 12), for example] was carefully re-assigned by Tellinghuisen (13); the other two regions around  $18\,908\text{ cm}^{-1}$  ( $5287\text{ \AA}$ , Ar<sup>+</sup> laser), and  $18\,830\text{ cm}^{-1}$  ( $5308\text{ \AA}$ , Kr<sup>+</sup> laser) are identified in the atlas ( $18000\text{--}19000\text{ cm}^{-1}$ ) recently published by Simons and Hougen at the National Bureau of Standards (14).

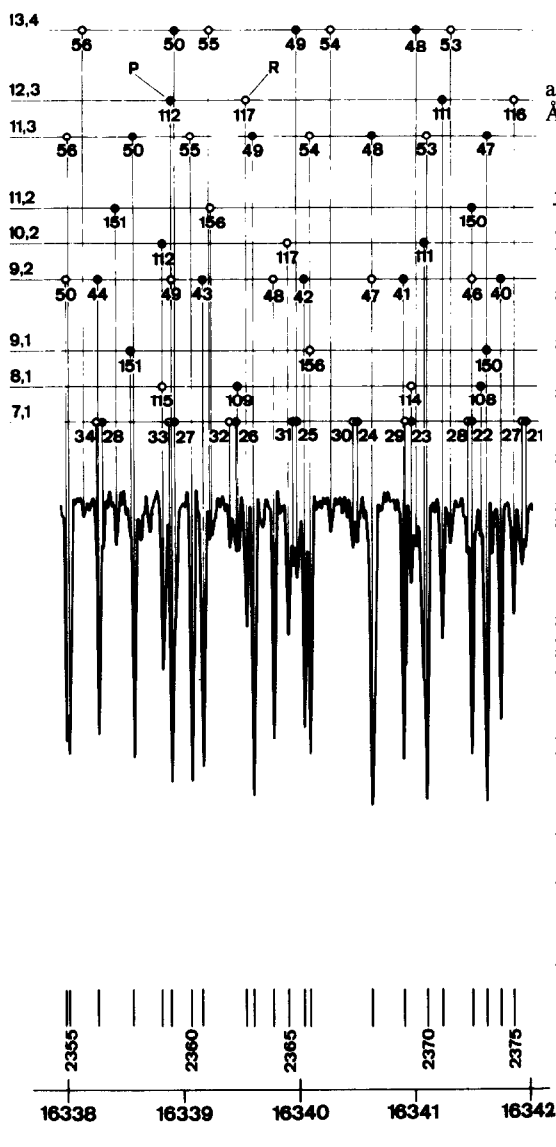


FIG. 6. Assignments of the iodine absorption lines in the vicinity of the He-Ne laser line  $\lambda = 6119 \text{ \AA}$  ( $\sigma = 16\,340 \text{ cm}^{-1}$ ).

TABLE VI

Observed and Calculated Wavenumbers around  $\sigma = 16\,340 \text{ cm}^{-1}$  (He-Ne,  $\lambda = 6119 \text{ \AA}$ )

No	$\sigma \text{ (cm}^{-1}\text{)}$	I	Assignments	$\sigma \text{ (cm}^{-1}\text{)}$
Atlas	(observed)			(calculated)
2354	16337.9936	41	50R (9,2)	16337.9924
2355	16338.0198	43	56R (11,3)	16338.0202
			56R (15,4)	.1429
			34R (7,1)	.2529
2356	.2701	40	44P (9,2)	.2703
	.3052	9	28P (7,1)	.3018
	.4165	8	151P (11,2)	.4188
2357	.5740	44	50P (11,3)	.5727
			151P (9,1)	.6280
2558	.7098	6		
	.8223	29	112P (10,2)	.8180
			115R (8,1)	.8258
			33R (7,1)	.8562
			27P (7,1)	.8633
2359	.9008	48	49R (9,2)	.9010
			112P (12,3)	.9298
			50P (13,4)	.9411
2360	16339.0755	48	53R (11,3)	16339.0731
2361	.1739	45	43P (9,2)	.1725
	.2462	6	156R (11,2)	.2591
	.4031	8	32R (7,1)	.4007
			26P (7,1)	.4460
	.4801	9	109P (8,1)	.4764
2362	.5528	22	117R (12,3)	.5507
2363	.6171	50	49P (11,3)	.6144
2364	.7897	40	48R (9,2)	.7903
2365	.9142	23	117R (10,2)	.9115
			31R (7,1)	.9464
	.9908	13	25P (7,1)	.9900
			49P (13,4)	16340.0080
2366	16340.0566	38	42P (9,2)	.0554
2367	.1064	43	156R (9,1)	.1051
			54R (11,3)	.1061
	.2834	6	54R (13,4)	.2876
	.4790	8	30R (7,1)	.4732
	.5150	7	24P (7,1)	.5152
2368	.6439	52	48P (11,3)	.6363
			47R (9,2)	.6602
			29R (7,1)	.9813
2369	.9197	44	41P (9,2)	.9190
	.9831	14	114R (8,1)	.9877
			23P (7,1)	16341.0216
			48P (13,4)	.0543
			111P (10,2)	.0856
2370	16341.1219	51	53R (11,3)	.1192
2371	.2539	24	111P (12,3)	.2528
	.3265	8	53R (13,4)	.3294
	.4738	9	28R (7,1)	.4705
2372	.5117	43	22P (7,1)	.5091
			46R (9,2)	.5109
			150P (11,2)	.5317
2373	.6399	51	108P (8,1)	.6295
			47P (11,3)	.6384
			150P (9,1)	.6530
	.6876	9		
2374	.7636	37	40P (9,2)	.7633
	.8737	20	116R (12,3)	.8720
	.9461	11	27R (7,1)	.9410
	.9791	8	21P (7,1)	.9780

### 3.1. The Spectral Region around $19\,429.8 \text{ cm}^{-1}$ ( $5145 \text{ \AA}$ , Ar<sup>+</sup> Laser)

(a) Comparison between the assignments based on the molecular constants determined by Wei and Tellinghuisen (10), and those deduced from Fourier spectroscopy. Inspection of Table VII shows the improvements reached by the Fourier spectroscopy measurements in the region around  $19\,429.8 \text{ cm}^{-1}$ . The agreement between observed and calculated wavenumbers is, in general, good especially for unperturbed single lines as, for example, the intense rotational line (44,0)R(50) [Fig. 7, Table VII (where  $\sigma_{\text{cal}} - \sigma_{\text{obs}} \approx 0.001 \text{ cm}^{-1}$ )]. The assignments differ

TABLE VII

Comparison between Wavenumbers Calculated with Different Sets of Constants in the Vicinity of the Ar<sup>+</sup> Laser Line  $\lambda = 5145 \text{ \AA}$  ( $\sigma = 19\,429.8 \text{ cm}^{-1}$ )

Band $v', v''$	Line	Int. Obsr. [1]	Wavenumber $\sigma \text{ (cm}^{-1}\text{)}$				$(J_{\text{max}})$ [9]	
			Observed	Calculated				
			Fourier Spectroscopy [1]	Fourier Spectrosc. [5]	Wei [10] Tel. [13]	Barrow Yee [9]		
46,0	R (80)	63	19429.1831	.1837		.17	94	
43,0	P (14)	74	.2612	.2582	.27	.24	60	
43,0	R (16)			.2672	.28	.25		
49,1	P (27)	21	.3184	.3160	.30	.33	82	
52,0	R (119)	25	.3770	.3900	.87	(30.150)	64	
44,0	R (50)	72	.4501	.4491	.46	.44	68	
60,2	R (49)			.4810	.44	.56	67	
51,1	R (60)	20	.5085	.5088	.48	.50	62	
44,0	P (48)	77	.6064	.6040	.62	.60	68	
49,0	P (103)			.6156	.70	.71		82
60,2	P (48)			.6680	.63	.75	67	
58,1	R (98)	12	.7382	.7359	.94	.61	62	
61,2	R (54)			.8050	.76	.84	62	
43,0	P (13)	74	.8204	.8157	.83	.80	60	
43,0	R (15)			.8250	.84	.81		
50,1	P (46)	61	.9343	.9267	.91	.93	50	
47,0	P (88)			.9362	.95	.91		99
49,1	R (28)	16	.9997	.0020	.98	.01	82	
46,0	P (78)	64	19430.0505	.0505	.06	.03	94	
57,1	R (95)			.0617	.17	.14		59
50,0	R (110)	34	.1107	.1069	.31	(29.650)	50	
62,2	R (56)	25		.138	.10	.17	66	
52,1	R (65)			.1491	.146	.12	.13	64
57,1	P (94)				.151	.22	.19	59
58,1	P (97)				.176	.32	.03	62
61,2	P (53)				.184	.15	.22	62

slightly from those deduced from the molecular constants published by Wei and Tellinghuisen (10). For example, the line (58,1) R(98) is now correctly assigned. In this region five pairs of lines, namely, the pairs [(43,0) P(14), R(16)], [(43,0) P(13), R(15)], [(50,1) P(46), (47,0) P(88)], [(44,0) P(48), (49,0) P(103)], and [(46,0) P(78), (57,1) R(95)], coincide within  $0.010 \text{ cm}^{-1}$  (see column 5, Table VII). Now if we consider the calculated wavenumber based on the molecular constants given by Wei and Tellinghuisen (10), one notes that the calculated distances be-



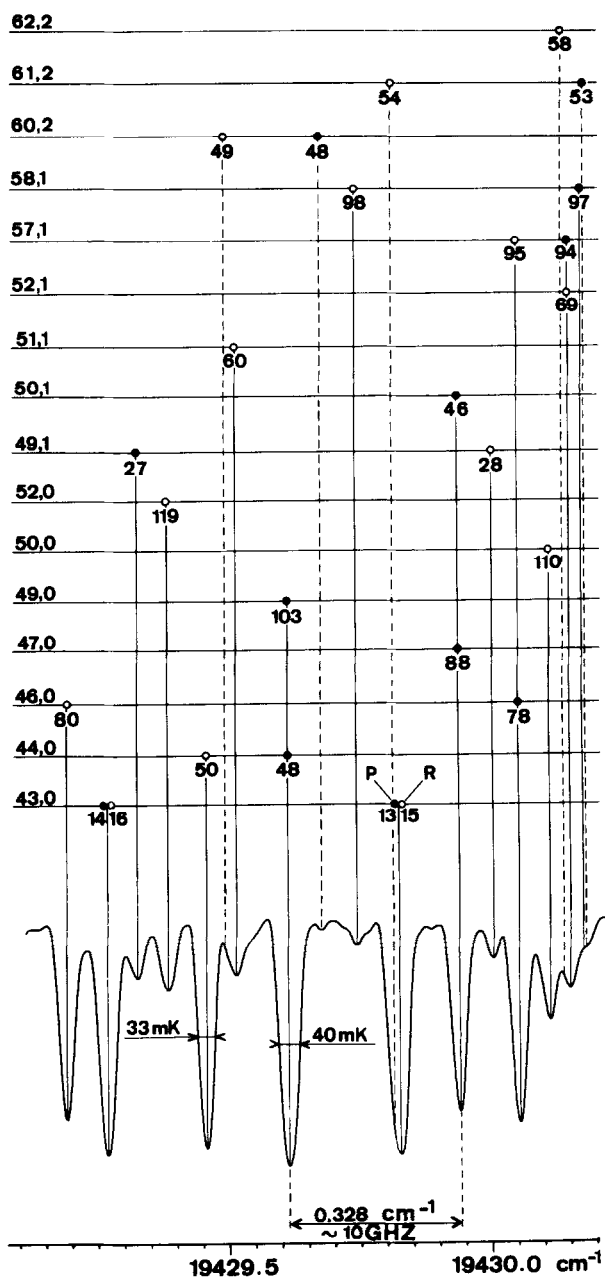


FIG. 7. Assignments and widths of the iodine absorption lines in the vicinity of the  $\text{Ar}^+$  laser line  $\lambda = 5145 \text{ \AA}$  ( $19\,429.8 \text{ cm}^{-1}$ ). The distance between the two complex lines [ $P(48)$ ,  $P(103)$ ] and [ $P(88)$ ,  $P(46)$ ] is found to be  $0.328 \text{ cm}^{-1}$  or  $\sim 10 \text{ GHz}$  [see Ref. (17)].

tween the lines of each pair increase with the  $J$  values of the rotational lines involved in these pairs: for the [ $P(14)$ ,  $R(16)$ ] and the [ $P(13)$ ,  $R(15)$ ] pairs of lines the calculated separations are  $0.010 \text{ cm}^{-1}$  in agreement with our estimate, but the

TABLE VIII

Doublets Splittings Measurements: Comparison between Fabry-Perot Measurements (17) and Fourier Measurements

Absorbed lines [17]	Assignments of the fluorescence doublets [13][16][17]	Doublet splittings (cm <sup>-1</sup> )		
		Fabry-Perot Data	Fourier Data	
		Measured [17]	Measured [1]	Calculated [5]
44,0 P (48)	44,0 P (48) R (46)	7.1 ± 0.3	7.085	7.085
49,0 P (103)	49,0 P (103) R (101)	15.3 ± 0.3	15.270	15.258
58,1 R (98)	58,1 R (98) P (100)	14.8 ± 0.3	14.767	14.782
43,0 P (13)	43,0 P (13) R (11)	1.87 ± 0.3	1.858	1.866
43,0 R (15)	43,0 R (15) P (17)	2.46 ± 0.3	2.454	2.462
47,0 P (88)	47,0 P (88) R (86)	13.1 ± 0.3	13.036	13.035

separations for the pairs  $[P(46), P(88)]$ ,  $[P(48), P(103)]$ , and  $[P(78), R(95)]$ , would be 0.040, 0.080, and 0.110 cm<sup>-1</sup>, respectively. [In fact, the recorded half-widths of the spectral lines in this region (Fig. 7) have a maximum value of 0.040 cm<sup>-1</sup>, of which the hyperfine structure contributes about 0.025–0.030 cm<sup>-1</sup> (11, 15)]. This is a good illustration of the observation made in Section 2, viz., that at the head of the bands (low  $J$ ) the discrepancy is low and nearly constant, following which it increases continuously with  $J$ . Finally it can be noted that using a monomode Ar<sup>+</sup> laser the rotational line (49,1)  $R(28)$  cannot be easily excited simultaneously with the composite line [(50,1)  $P(46)$ , (47,0)  $P(88)$ ], which is located 0.065 cm<sup>-1</sup>, toward the lower wavenumbers.

(b) Comparison between the assignments based on the molecular constants determined by Barrow and Yee (9), and the assignments deduced from Fourier spectroscopy. Other molecular constants describing the B-X system of I<sub>2</sub> were published by Barrow and Yee (9). The wavenumbers calculated by means of these constants, which are listed in Table 2 of Ref. (9), are given in Table VII, column 7. When the  $J$  values of the transitions are below the maximum  $J$  values identified in each band by these authors [ $J_{\max}$  of Table I of Ref. (9), and reproduced in column 8, Table VII of the present work], then the differences between the observed Fourier wavenumbers (column 4) and those calculated using the absorption data of Barrow and Yee (column 7) do not exceed ±0.020 cm<sup>-1</sup>. However, for  $J$  values higher than those  $J_{\max}$  values, the discrepancies increase rapidly; for example, for the lines (57,1)  $P(94)$ , (57,1)  $R(95)$ , (58,1)  $P(97)$ , (58,1)  $R(98)$ , (49,0)  $P(103)$ , (50,0)  $R(110)$ ,

and (52,0)  $R(119)$  the discrepancies are  $-0.040$ ,  $-0.090$ ,  $+0.140$ ,  $+0.130$ ,  $-0.090$ ,  $+0.460$ , and  $-0.770$   $\text{cm}^{-1}$ , respectively. Therefore, the use of the constants of Barrow and Yee has to be limited to the maximum  $J$  values of each band observed by these authors. Since the molecular constant  $H'_v$  has been neglected in their study, the extrapolation to high  $J$  values remains questionable and, in any case, has to be made with extreme caution. For instance, in the recent laser fluorescence studies [Clark and McCaffery (16)] the assignments of the fluorescence series, although correct, are given for two of them with wrong wavenumbers: the wavenumbers of the observed transitions (49,0)  $P(103)$  and (58,1)  $R(98)$  must be inverted, as can be seen by inspection of Table VII. These misassignments have, obviously, their origin in the use and the extrapolation to relatively high  $J$  values, of the data of Barrow and Yee. [Another fluorescence series (61,2)  $P(54)$  is given in Ref. (16); it should be (61,2)  $R(54)$ , which is in agreement both with our assignments (Table VII), and with their own observations; see Fig. 2 of Ref. (16).]

(c) *Comparison between fluorescence doublet splittings measurements by means of a Fabry-Perot interferometer and doublet measurements obtained by Fourier spectroscopy.* In view of the precise nature of the data obtained by Fourier spectroscopy it is also now possible to give a comprehensive interpretation of the fluorescence doublet measurements, in this region, made by Patterson *et al.* using a Fabry-Perot interferometer (17). Table VIII contains the splittings of the six doublets observed by these authors (17) and their corresponding assignments. The agreement between the measured splittings (column 3, Table VIII) with those calculated by means of our molecular constants (5), or with those obtained from the observed wavenumbers (1) of the doublet components, is excellent.

Again, in the experiment of Patterson *et al.* (17) the separation between the lines (44,0)  $P(48)$  and (49,0)  $P(103)$  is found to be of the order of 571 MHz ( $0.019$   $\text{cm}^{-1}$ ) in agreement with our observation; Clark and McCaffery found them to be about  $0.110$   $\text{cm}^{-1}$  apart, a value not compatible with the half-width ( $0.040$   $\text{cm}^{-1}$ ) of the complex line  $P(48) P(103)$  recorded in our spectrum (see Fig. 7).

Finally, for completeness and to conclude the discussion of the assignments of the iodine lines in this spectral region, Table VII and Fig. 7 also contain transitions (dashed lines) connected to the "hot" band  $v'' = 2$ . These bands, very weak in our experimental conditions (1, 18), were not analyzed; only the calculated wavenumbers are given here; transitions belonging to the  $(v', 2)$  bands with  $v' > 62$  were not searched, our assignments being limited to  $v' = 62$ .

### 3.2. The Spectral Regions around $18\,908$ $\text{cm}^{-1}$ ( $5287$ Å, $\text{Ar}^+$ Laser) and $18\,830$ $\text{cm}^{-1}$ ( $5308$ Å, $\text{Kr}^+$ Laser)

In these two regions the number of recorded lines by Fourier spectroscopy is about 30% higher than those recorded in the spectrum published by Simons and Hougen (14). Of course, the 30% additional lines are weak and are in general close to intense lines: the lines could be detected because of the high instrumental resolving power used, which was of the order of  $10^6$ .

For the  $(v', 0)$  transitions, the assignments of Simons and Hougen agree completely with ours. Moreover, recently we were made aware of the Franck-Condon

factors calculated by Tellinghuisen (18). Consequently, we have systematically searched in these two regions for the lines belonging to the bands ( $v',v''$ ) with  $28 \leq v \leq 46$  and  $v'' = 2$ . For these bands the Franck-Condon factors should be high enough so that transitions belonging to the bands ( $v',2$ ) would be detectable in our spectrograms. Indeed, we find these bands and the identification of the corresponding lines is given in Fig. 2, Table II and Fig. 4, Table IV.

In conclusion, we wish to point out that assignments in other regions of the iodine absorption spectrum can be made equally well with the use of the molecular constants deduced (5) from our Fourier spectroscopy measurements.

#### ACKNOWLEDGMENTS

We wish to express our gratitude to A. Raynal and D. Merle, who helped us to achieve the present work. We are much obliged to H. Calvignac, B. Desmarests, and M. Rey for having prepared the graphs and tables. We also thank Professors H. Stroke and K. Narahari Rao for kindly reading this manuscript, and Dr. R. Bacis for giving us valuable comments.

RECEIVED: October 5, 1978

#### REFERENCES

1. S. GERSTENKORN AND P. LUC, "Atlas du spectre d'absorption de la molécule de l'iode," 14 800–20 000 cm<sup>-1</sup>, Editions du CNRS, Paris, 1978.
2. R. L. BYER, R. L. HERBST, H. KILDAL, AND M. D. LEVENSON, *Appl. Phys. Lett.* **20**, 463–466 (1972).
3. B. WELLEGEHAUSEN, K. A. STEPHAN, D. FRIEDE, AND H. WELLING, *Opt. Commun.* **23**, 157–161 (1977).
4. J. B. KOFFEND AND R. W. FIELD, *J. Appl. Phys.* **48**, 4468–4472 (1977).
5. P. LUC, *J. Mol. Spectrosc.* to appear.
6. S. GERSTENKORN, P. LUC, AND A. PERRIN, *J. Mol. Spectrosc.* **64**, 56–69 (1977).
7. R. J. LEROY, *J. Chem. Phys.* **52**, 2683–2689 (1970).
8. J. D. BROWN, G. BURNS, AND R. J. LEROY, *Canad. J. Phys.* **51**, 1664–1678 (1973).
9. R. F. BARROW AND K. K. YEE, *J. C. S. Faraday II* **69**, 684–700 (1973).
10. J. WEI AND J. TELLINGHUISEN, *J. Mol. Spectrosc.* **50**, 317–332 (1974).
11. M. D. LEVENSON, Thesis, Stanford University, 1971.
12. M. BROYER, J. C. LEHMAN, AND J. VIGUE, *J. Physique* **36**, 235–241 (1975).
13. J. TELLINGHUISEN, *J. Mol. Spectrosc.* **62**, 294–295 (1976).
14. J. D. SIMONS AND J. T. HOUGEN, *J. Res. Nat. Bur. Standards Sect. A* **81**, 25–80 (1977).
15. M. KROL AND K. K. INNES, *J. Mol. Spectrosc.* **36**, 295–309 (1970).
16. R. CLARK AND J. McCAFFERY, *Mol. Phys.* **35**, 609–615 (1978).
17. G. D. PATTERSON, S. H. DWORETSKY, AND R. S. HOZAK, *J. Mol. Spectrosc.* **55**, 175–181 (1975).
18. J. TELLINGHUISEN, *J. Quant. Spectrosc. Radiat. Transfer* **19**, 149–161 (1978).